A CLASSIFICATION OF UNIQUELY DIFFERENT TYPES OF NUCLEAR FISSION GAS BEHAVIOR

GERARD L. HOFMAN and YEON SOO KIM*
Nuclear Engineering Division, Argonne National Laboratory
9700 South Cass Avenue, Argonne, IL 60439-USA
*Corresponding author. E-mail : yskim@anl.gov

Received July 11, 2005

The behavior of fission gas in all major types of nuclear fuel has been reviewed with an emphasis on more recently discovered aspects. It is proposed that the behavior of fission gas can be classified in a number of characteristic types that occur at a high or low operating temperature, and/or at high or low fissile burnup. The crystal structure and microstructure of the various fuels are the determinant factors in the proposed classification scheme. Three types of behavior, characterized by anisotropic α-U, high temperature metallic γ-U, and cubic ceramics, are well-known and have been extensively studied in the literature. Less widely known are two equally typical low temperature kinds: one associated with fission induced grain refinement and the other with fission induced amorphization. Grain refinement is seen in crystalline fuel irradiated to high burnup at low temperatures, whereas breakaway swelling is observed in amorphous fuel containing sufficient excess free-volume. Amorphous fuel, however, shows stable swelling if insufficient excess free-volume is available during irradiation.

KEYWORDS : Nuclear Fuel, Fission Gas, Fuel Swelling, Grain Refinement, Rim Effect, Amorphization, Free Volume

1. INTRODUCTION

Of the various irradiation performance issues of nuclear fuels, the behavior of the noble fission gases, Xe and Kr, is often the issue that determines the useful in-reactor life or fissile burnup capability of a particular fuel type and design. These gases, being largely insoluble in all forms of fissile material, tend to precipitate into gas bubbles and are the main cause of fuel swelling. The magnitude of swelling and the capability of fission gas to escape from the fuel interior depend primarily on the gas bubble morphology that develops during irradiation. In addition to the main operating parameters, i.e., temperature and fission rate, many minor variables determine fission gas behavior. The physical form of the fuel, fabrication variables and impurity levels may all affect the evolution of the fission gas bubble morphology. Nevertheless, experience has shown that there are a few major types of behavior that permit the construction of some form of classification scheme. This is what has been attempted in the present paper (see Table 1).

Several of the classes of behavior outlined in the present scheme have been thoroughly studied and documented in the literature of the past half century. Two that stand out are metallic uranium and uranium dioxide; to a much lesser extent are such related ceramic compounds as uranium carbide and nitride. Because of the abundant literature on these fuel types, we will only mention their chief attributes and irradiation behavior here for the sake of completeness in proposing our classification scheme. We will concentrate the discussion on two particular types of fuel behavior, i.e., grain refinement and amorphization, as these topics have not been treated in the context of fuel in general.

2. HIGH TEMPERATURE BEHAVIOR

2.1 Uranium Metal

Uranium metal is the obvious "perfect" fuel. No other form of uranium than the metal itself possesses better properties for the reactor designer. It was, therefore, pursued as a reactor fuel during the early years of reactor development. Irradiation experiments, however, soon revealed its limitations. In the operating temperature range for most of its applications, uranium exists in an anisotropic (orthorhombic) crystal structures the α-U phase. Temperatures

· Argonne National Laboratory's work was supported by the U.S. Department of Energy, Office of International Policy and Analysis (NA-241), National Nuclear Security Administrative, under contract W-31-109-Eng-38.

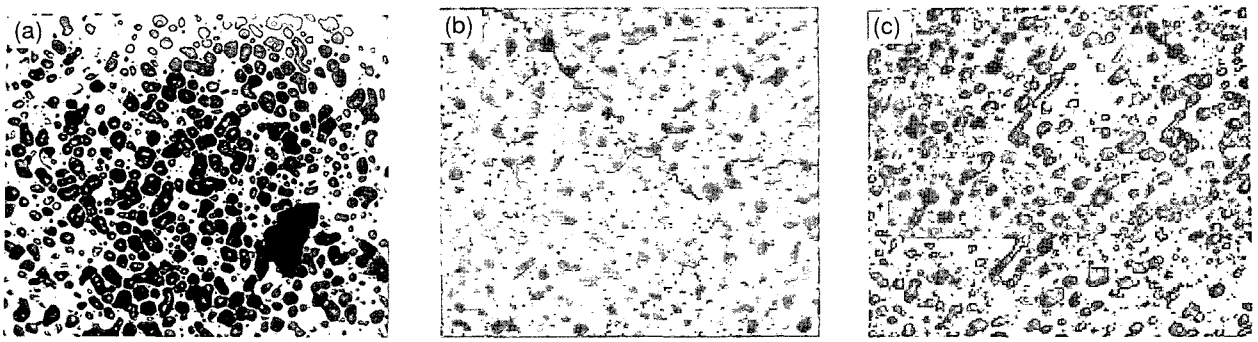

Fig. 1. Gas Bubble Morphology of γ-U Irradiated to 1 - 2x10^{21} Fiss/cm^3 at Temperatures Where γ-phase is the Equilibrium Phase (600°C < T): (a) γ-U Metal (optical), (b) U-10Zr (SEM, As-polished), (c) U-8Mo (Optical)

above 776° C the equilibrium phase is the BCC γ-U phase.

2.1.1 α-U

The most important irradiation characteristic of α-uranium is its dimensional instability in the form of anisotropic growth and swelling, resulting from the anisotropic properties of the orthorhombic crystal structure. This anisotropic volume increase in individual grains in a polycrystalline sample results in shape changes and, therefore, in mismatched strains between the individual grains. The stress developed due to these mismatched strains can be released by plastic deformation at the grain boundaries, commonly referred to as 'tearing' or 'cavitation'. A typical cavitational swelling morphology shows a very deformed 'swirled' microstructure. Cavitational swelling is not fission gas driven and is basically a process which occurs at relatively low temperatures (in the range of 400° C - 600° C). Because the cavities are practically empty, cavitational swelling is relatively compressible so that, if cladding restraint is provided, it can be suppressed. However, at higher burnup, fission gas will collect in the preformed cavities, pressurize them and impart bubble-like properties to them. Unless the fission gas can escape, the buildup of internal pressure will make the fuel less compressible.

2.1.2 Low alloy U

The cavitational swelling can be reduced by addition of a small amount of elements such as Fe, Mo, Al and Si [1]. The role of alloying elements in solid-solution or finely dispersed coherent precipitates is to inhibit the migration of either interstitials to dislocations or vacancies to voids and thus promoting recombination of the defects. An alternative theory is that alloying additions interfere with the formation and movement of dislocation loops. The result of either model is reduction in swelling by void forming processes, and suppression of anisotropic growth. In general, uranium alloys have more uniform microstructural distribution of cavities than un-alloyed uranium, which implies a lesser degree of cavity formation at grain or twin boundaries in the alloys. This may be a result of the generally finer grain and subgrain structure of the dilute alloys, which produces greater formation of intragranular pores of the alloys. Even with these alloy adjustments, α-U is applicable as a low burnup fuel, and because of its anisotropic characteristics it represents a unique type of behavior compared to alloys and compounds.

2.1.3 γ-U

Unlike the cavitational swelling of α-U, swelling of γ-U is predominantly due to the growth of fission gas bubbles. Its fission gas behavior is characterized by high mobility at the relatively high temperatures where it exists as the equilibrium uranium phase. Because of high diffusivities, fission gas bubble swelling rates of metallic U are high even at the relatively low burnup levels. Some degree of swelling rate reduction can be achieved by alloying with elements that have a high degree of solubility in the γ-phase e.g. Mo, Zr and Nb. However, high burnup performance can only be achieved by releasing the fission gas from the internal porosity. Some examples of this type of fission gas behavior are shown in Fig.1.

3. CUBIC CERAMIC FUELS

This class of fuels is characterized by retaining their identifiable, by any currently available experimental method, crystalline structure during the on-going fissioning process. As early as 1960, Berman et al. [2] established a correlation between crystal stability and crystal symmetry. Their results suggested that only material with crystal structures other than cubic lose crystalline x-ray diffraction patterns after fission damage. The "fission stable" cubic uranium compounds appeared to behave in a predictable manner: therefore, they are well suited for high temperature applications. The fission gas behavior of this class of fuels follows the classical "Booth model," well established in treating the formation of irradiation induced defects and

fission gas bubbles in the fuel matrix and on the grain boundaries. Its various refinements have been extensively reviewed over the last few decades [3,4] and will therefore not be repeated in the present paper. Except for very high temperature effect such as grain growth, and gas bubble movement in high temperature gradients (UO_2), the basic gas bubble morphology is shown in Fig.2 for UO_2: This morphology is representative of type "A" behavior as identified in Table 1.

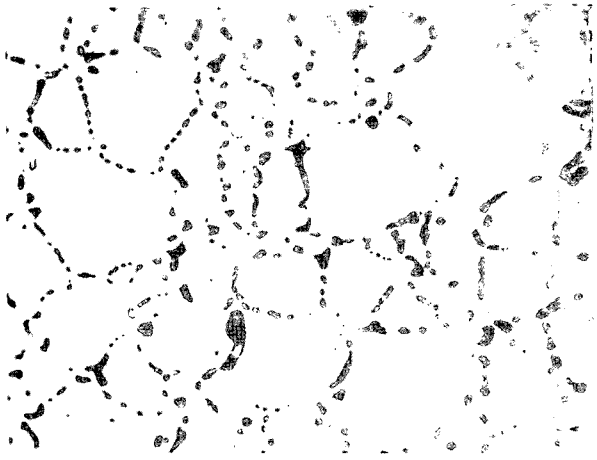

Fig. 2. Structure of UO_2 Irradiated at 1400°C to a Burnup of $1.5x10^{20}$ fiss/cm^3 [5]

4. LOW TEMPERATURE BEHAVIOR

4.1 Crystalline Fuels

The classic model served the observed fuel behavior, of particular UO_2, rather well until a high burnup effect was identified in high-burnup tests of power reactor fuels. Because of the thermal neutron flux shape and the buildup of Pu at the periphery of UO_2 pellets of light water reactor fuel rods, the fission damage is concentrated there. During examination of high burnup tests it became clear that this radial peripheral region of high burnup fuel rods had undergone a profound change. This change, coined "rim effect" by the light water reactor fuel community, consists of a transformation of the original ~5 μm grain size of the

Table 1. Fuel Behavior Classification

Operational Parameter / Major Fuel Group	Classification of major uranium fuels with respect to fission gas behavior			
	Low temperature		High temperature	
	Low-med Bu	High Bu	Low-Med Bu	High Bu
Ceramics UO_2, UN, UC	Classic (A) behavior, gas bubble growth on grain boundaries (G.B.), low gas release	Grain (D) refinement, gas bubble growth on new G.B.	As at low (A) temperature, grain growth and columnar grain formation in UO_2, higher gas release	G.B. bubble (A) interconnection, gas release
Metallic U and low alloys	α-U (B) Anisotropic growth, cavity swelling, improved behavior with minor alloy additions - Al, Si, Fe, Mo	Not usable	γ-U (E) High gas mobility, bubble interconnection, high break-away swelling, gas release	The same as left (E)
γ-U alloys U-Mo, U-Zr, etc	Classic behavior, (A) gas bubble growth on G.B.	Grain refinement, (D) gas bubble growth on new G.B.	Similar to γ-U (E)	The same as left (E)
Intermetallics U_3Si_2, UAl_x, etc	Amorphization (C) (C-1) Low free volume: small uniform bubble morphology, stable	Amorphization Continued growth of uniform stable morphology	Similar to γ-U (E) crystalline	The same as left (E)
U_3Si, U_6Fe, etc	(C-2) High free volume: larger non uniform bubble morphology	Bubble interconnection break-away swelling	Similar to γ-U crystalline	Similar to γ-U crystalline

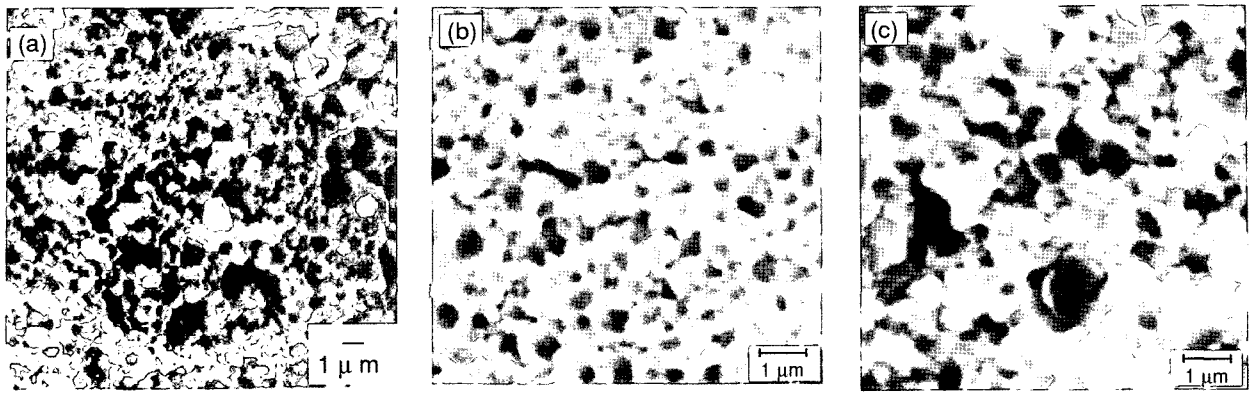

Fig. 3. SEM Images of Fracture Surfaces of (a) UO_2 Irradiated to ~80 GWd/MTU [9], (b) U-Mo Irradiated to ~150 GWd/MTU, (c) U_4O_9 Irradiated to ~90 GWd/MTU

UO_2 fuel into a very refined grain structure with a grain size of ~0.2 μm. The enormous increase in grain boundary areas in this refined grain structure provides a concomitant increase in sites for gas bubble nucleation and growth.

In retrospect, Berman et al [6] and Lambert [7] had earlier identified this irradiation effect in UO_2 and (U-Pu) O_2 fuels irradiated to high burnup. The so-called extended burnup program for light water reactors thus rediscovered it. Also, in a 1986 paper on an irradiation if uranium oxide dispersed in Al Hofman [8] revealed a clear comparison between the early indications of Berman and Lambert and that of the by then available, Scanning Electron Microscopy (SEM) of irradiated uranium oxide. This appeared to lead to a consistent interpretation of the rim effect. So far all observations of the phenomenon of grain refinement were made on UO_2. It was to say "surprising" when one of the present authors observed a microstructure in an irradiated γ-phase U-Mo alloy that appeared to be very similar to that of uranium oxide. The fuel fracture surfaces of the different fuels are compared in Fig 3 and speak for themselves. What is so remarkable is the observation that these very different materials exhibit such a similar final microstructure after essentially similar degrees of fission damage. This fission induced change in fuel microstructure is identified as behavior type "D" in Table 1.

Such a microstructural evolution recalls the results of extensive work on "dynamic recrystallization" in heavily deformed metals. Following the work in this area, it is not a great leap to draw the analogy between deformation induced and fission induced dislocation behavior. However, because of the complexity of the fuel materials considered, one should not hope to proceed beyond a phenomenological or semi-mechanistic treatment of the phenomenon. Nevertheless, we should like to offer the following observations and deductions to, hopefully, aid in the more complete physical description of this aspect of fuel behavior.

1) Let us first recall the chronology of the observations of Grain Refinement, Recrystallization, or Rim Effect, as the phenomenon in variously referred to.

1963 - Berman UO_2,	[6]
1968 - Lambert ($UPuO_2$)	[7]
1986 - Hofman (U_4O_9)	[8]
1988 - Stehle (UO_2)	[10]
1991 - Walker et al. (UO_2)	[9]
1992 - Cunningham et al. (UO_2)	[11]
1992 - Thomas et al. (UO_2)	[12]
1999 - Hofman et al. (U-Mo)	[13]

i. It appears that the common factors in these observations are: relatively low temperature at which fission (or radiation) effects dominate the microstructural behavior; approximately below a homologous temperature of $0.4T_m$.

ii. The persistent existence of high dimensional crystal structure of the fuel regardless of the level of fission damage incurred.

iii. A certain, high, level of damage at which "grain refinement" occurs.

It is perhaps coincidental that UO_2 with a FCC ceramic CaF structure and a melting point of 2850°C; and U-Mo alloy with a BCC transition metal alloy structure having a melting point of 1140°C exhibit a very similar recrystallized grain structure after ~70 MWd/MTU. We think, however, that a case can be made for the analog with mechanical deformation. As long as the fuel retains its crystalline structure, the basic (classical) damage generation consists of point defects and point defect clusters that form dislocation loops which evolve into interacting dislocations. The evoluation of fission induced generation of dislocations and their interaction, although different in origin, may have similarities in its progression to that which takes place in the case of deformation.

Because of its practical value, many analyses have been done in the case of dynamic recrystallization of metals,

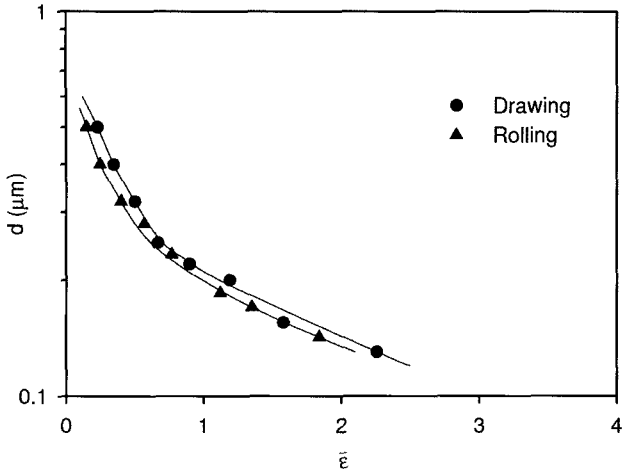

Fig. 4. Dislocation Cell Diameter in Cold Worked Nb [14]

proving this to be a complex issue. We only address here the seemingly related metallurgical processes involved in the mechanical and in-reactor conditions that lead to "grain refinement". We are convinced that it is a daunting task to mechanistically model this aspect of irradiation behavior given the multitude of uncertainties existing even in the out-of-reactor analysis, not to mention the in-pile complexities. However, a phenomenological description appears within reach and perhaps illuminating as well.

Most metals develop a cellular dislocation substructure during cold deformation. In BCC metals with a high stacking fault energy this substructure is established at low strains of ~10% and consists of three-dimensional tangled dislocation walls surrounding areas of low dislocation density. The work hardening obeys the Taylor relation between the flow stress, τ, and the dislocation density, ρ, $\tau = A\ G\ b\ \rho^{1/2}$, where A is a material constant, G, the shear modules and b the Burgers vector. With further deformation the size of the cells decreases, the walls become sharper and the interior of the cells contains progressively fewer dislocations. The cell size, d, is related to the dislocation density as $d=k\rho^{-1/2}$. The average cell size becomes quite small at larger amounts of strain as shown in Fig.4 for Nb - a high stacking fault energy metal similar to (γ)U-Mo. The concentration of dislocations into an increasing cell boundary area has been described as a mechanism of minimization of stored energy of deformation [15].

The sharpening of the cell boundaries at smaller cell sizes eventually leads to the conversion of cell boundaries into low-angle grain boundaries – a process that may be called "dynamic polygonization." The flow stress obeys the Hall-Petch relationship, $\tau = ad^{-1/2}$. Further deformation leads to the appearance of small strain-free grains with high angle boundaries, a process referred to as "dynamic recovery and recrystallization" [16-18]. The idealized evolution of the microstructure with increasing amount of cold work can be summarized as follows:

- Initial rapid multiplication of dislocation
- Formation of cellular dislocation structure
- Reduction of cell size and sharpening of cell boundaries with angles of ~ 1°
- Formation of subgrains (polygonization) with low angle boundaries < 10°
- Formation of new grains with high angle boundaries (recrystallization)

Following the analogy of this description, Rest and Hofman [19-21] developed a model for the microstructural evolution during fission damage accumulation in crystalline fuel, with the emphasis on UO_2. The key assumption in this model is that the dislocation generation during deformation may be replaced by the fission damage generation of dislocation loops.

We will now examine whether the experimental observation on irradiated fuel are consistent with the mechanical deformation description and model. The SEM fractographs of all experiments shown in Fig.3 lead to the conclusion that the fracture mode is intergranular and the facetted appearance of the individual grains indicate that the grain boundaries are predominantly high-angle. The etched surfaces in Berman's and Lambert's work are in accord with this observation. We may conclude that some form of recrystallization has occurred in all cases and that the grain boundaries are weakened by precipitated fission gas bubbles, and likely other fission products, as well.

This conclusion in itself is not inconsistent with the high-strain dynamic recrystallization stage in mechanical deformation. However, this tells us nothing about the evolution of the microstructure that leads to this final grain refinement. This requires experimental data on changes in mechanical properties and in the dislocation substructure. These data are very difficult to obtain on highly irradiation fuels and, except for some microhardness measurements, do not exist for the γ-U alloys. However, because of the recent interest in the high burnup rim effect in LWR fuel, several Transmission-Electron-Microscopy (TEM) examinations have been done on high burnup UO_2 samples.

Concerning the final grain refined structure, Ray et al. [22] determined the grain size distribution with TEM and found it similar to that measured on SEM fracture surfaces. However, Ray reports that the grain boundary angles are exclusively low angel (<5°) in the rim region. This observation supports the mircrostructural evolution through the polygonization stage and would refute recrystallization even though the local burnup of these particular samples reportedly exceeded 200 GWd/MTU.

Similarly, Sonoda et al. [23] report a low-angle subgrain structure in 90 GWd/MTU samples and support polygronization as the prime mechanism for grain refinement. In their discussion they do, however, suggest subsequent recrystallization without offering experimental proof.

On the other hand, Thomas et al [12] and Nogita et al. [24] report a mixture of low- and high-angle submicron

grains in rim region samples of ~ 100 GWd/MTU. These observations would support the further evolution of polygonized subgrains into recrystallized grains. However, Nogita found in addition a large number of very small (~20 nm) high angle grains in areas of high dislocation density. If these small high-angle grains, rather than the much larger low-angle subgrains, are the precursors to the final recrystallized grains, a mechanism similar to what occurs in high deformation bands in cold work metals is suggested as the final dynamic recrystallization stage.

Experimental data on the dislocation structure has only been reported in two of the above referenced TEM studies. The detailed evolution of the dislocation structure from fission generated dislocation loops is of course a key element of the grain refinement description and model. The initial stage of the R-H model [19] is based in part on early work by Whapham et al [25] on low burnup UO_2 irradiated at 400°C. A high density of interstitial loops (~10^{16} cm^{-3}) is first observed at a very low burnup of ~10^{-7} GWd/MTU. At ~10^{-2} GWd/MTU the loop density is ~$2x10^{16}$ cm^{-3} and the loop diameters vary in size from 5 to 40 nm. With increasing burnup these loops increase in size until they coalesce to form tangled dislocation networks evolving to a dislocation density of ~$2x10^{9}$ cm^{-2} at a burnup of 1 GWd/MTU with relatively defect free areas in between the dislocations.

The basic assumption in the R-H model is that this mechanism of dislocation accumulation continues to the vastly higher burnup levels where recrystallization occurs. The two TEM studies mentioned above lend some support to the assumption. Nogita et al [26] reports dislocation densities of ~10^{10} cm^{-2} at 6 GWd/MTU, increasing to ~$5x10^{10}$ cm^{-2} at 44 GWd/MTU, becoming more cellular in substructure. The dislocation density remains at this value in a rim sample at 85 GWd/MTU, albeit very inhomogeneous in distribution. In addition, interstitial loops of unspecified size and number were observed at 44 GWd/MTU. Ray et al. [27] report a dislocation density of ~$2.5x10^{10}$ cm^{-2} at ~60 GWd/MTU, outside the rim zone, as well as a density of $5x10^{14}$ cm^{-3} of 10-50 nm loops.

The average dislocation density in the "polygonized" rim zone was $5x10^{9}$ cm^{-2}. Both Nogita and Ray report the absence of loops in the rim zone. Considering the difficulties in measuring, in particular, inhomogeneous dislocation densities and the uncertainty in the precise TEM sample locations, we may conclude that those two observations are similar.

Spino et al [28,29] have attempted to extract information on the mechanism underlying grain refinement from UO_2 lattice parameter and microhardness changes. As shown in Fig.5, the lattice parameter as reported by Whapham [30] increases rapidly at low burnup as a result of the accumulation of interstitial loops. It soon returns to a lower value as the loops evolve into a dislocation network and, as Whapham shows, vacancy loops appear in the matrix. Spino's data show that at a higher burnup the lattice parameter again increases until grain refinement occurs in the rim region of the UO_2 LWR fuel pellets. The loop density of 5 x 10^{14} cm^{-3} reported by Ray above, when compared with Whapham's values of ~10^{16} cm^{-3}, would indicate that their effect on the increase in lattice parameter cannot be large.

There is a similar trend in the microhardness data shown in Fig.6. Several factors may contribute to these changes in addition to the involving dislocation structure, the most important of which are the changes in fuel chemistry when fission products accumulate with U burnup, and the evolution of fission gas porosity. Indeed, the drop in microhardness upon grain refinement can be largely explained by the attended increase in porosity as shown also for U-Mo fuel in Fig.7. Spino performed detailed analyses of the possible factors involved in the lattice parameter and microhardness changes and his conclusion appears to be qualitatively consistent with the R-H model.

The proceeding brief summary shows that the phenomenon of grain refinement is not fully understood. The

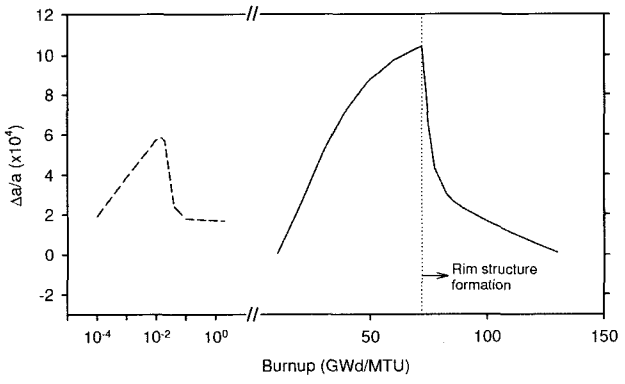

Fig. 5. Lattice Expansion and Contraction of Irradiated Fuels Relative to Unirradiated UO_2 as a Function of Local Burnup. The Solid Line is from Spino [28] and the Broken Line is from Whapham [30]

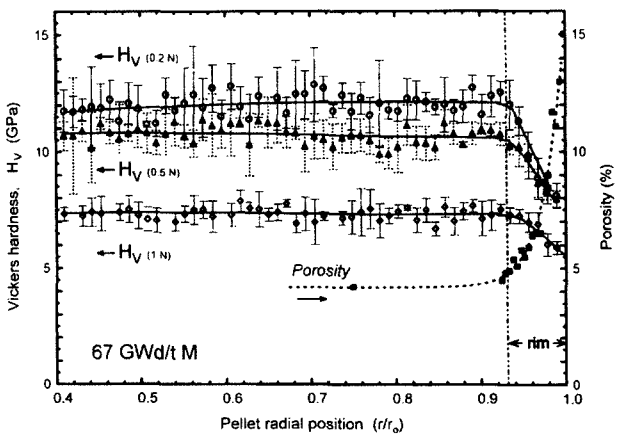

Fig. 6. Comparison of Microhardness and Porosity of Fuel [29]

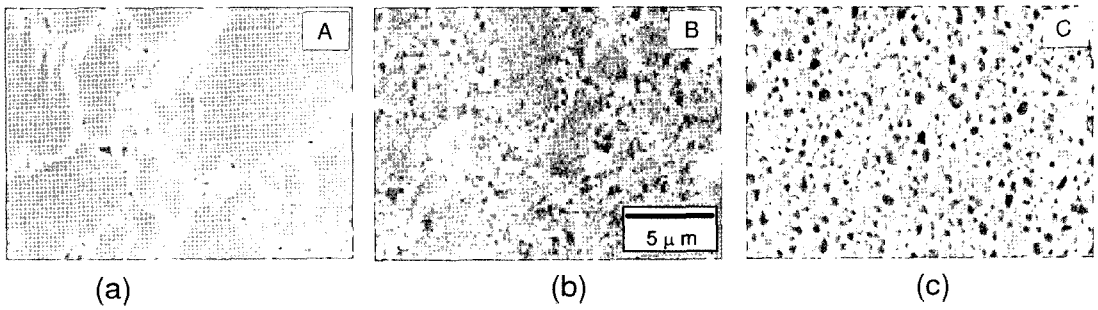

(a) Low burnup, only gas bubbles on grain boundaries, (b) medium burnup, grain refinement initiated, (c) high burnup, fully refined grains.

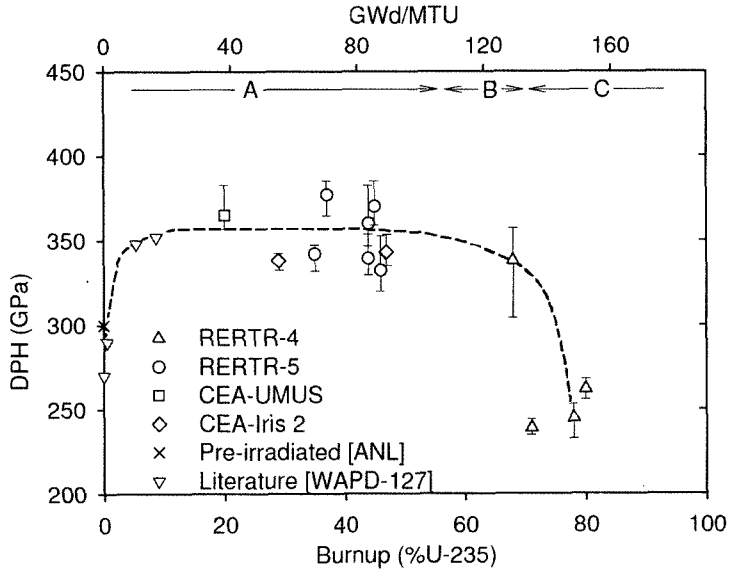

Fig. 7.U-Mo Microstructure and Microhardness Changes with Burnup. Microstructural Stages Classified as A, B, C in the Photos Correspond Respectively to the Regions in the Graph

available experimental evidence neither refutes nor satisfactorily supports the proposed description and models. However, we believe that the preponderance of the, albeit fragmentary, experimental observations favors the R-H model that, admittedly, is a simplification of the most complex reality.

Nevertheless, we concluded that the phenomenon of grain refinement can be classified as a general type of behavior at lower temperatures of fuels that retain a crystalline structure to high burnup indicated in Table 1 as type "D".

4.2 Non-Crystalline Fuels

By non-crystalline fuels we mean original normal crystalline fuel compounds or alloys that have evidently (as determined by x-ray or neutron diffraction) lost any degree of molecular order beyond next nearest neighbors, or, experimentally, crystalline volumes in excess of ~ 50 Å^3. A solid as such one could justifiably call amorphous or "glass-like" or perhaps nano crystalline, in any event, differs from the class of fuels discussed in the proceeding section that clearly retain their macro and micro crystallinity.

A large number and variety of compounds and alloys have been found to become amorphous when exposed to various types of irradiation. In fact, the original discovery of the phenomenon was made on naturally radioactive mineral crystals that were found to have "mictametized" as a result of α decay. In the case of fuel compounds the primary damage to the crystal structure is due to the highly energetic fission fragments. Amorphization is clearly a low temperature phenomenon as amorphized materials devitrify (recrystallize) at the so called glass transition temperature. Above this temperature, amorphization is not possible and the fuel in question has the familiar crystalline irradiation behavior. However, the behavior, particularly of fission gases, can be quite different in amorphized

fuels. For example, shown in Fig.8 are micrographs of two irradiated compounds, U_3Si and U_6Fe – desirable fuels because of their high uranium density. Both U_3Si and U_6Fe become amorphous at a relatively low damage dose [31,32]. The fission gas bubble morphology appears to be characteristic of that of alloys at high temperatures (compare with Fig.1)

Yet, these fuels were irradiated at ~100°C. Evidently the fission gas was highly mobile and the fuel material was easily deformed by the growing gas bubbles. Post-irradiation hardness tests showed that these fuels had retained their relatively hard and brittle pre-irradiation properties. The observed fluid-like behavior thus only exists during irradiation. Klaumunzer [33] has demonstrated this irradiation behavior with heavy ion beam irradiations of borosilicate glasses and Pd-Si metallic glasses. He was able to correlate the measured increase in fluidity in these tests with the excess free-volume that was independently measured on these glasses. Work on quenched metallic, glasses, has shown that the viscosity, η, during annealing tests can be described by the Doolittle equation [34].

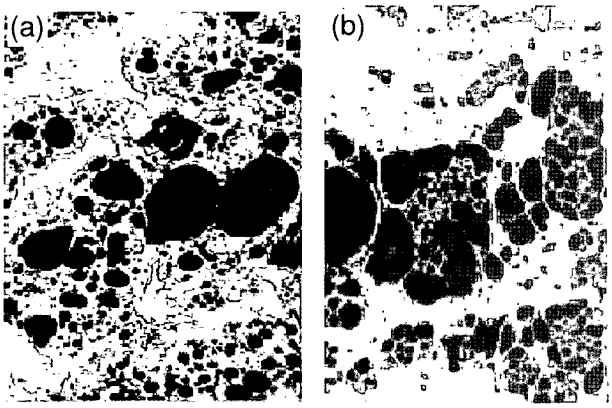

Fig. 8. Breakaway Swelling of Amorphous U-compounds. (a) U_3Si (8% total U burnup), (b) U_6Fe (17% total U burnup)

$$\eta = \eta_0 \exp\left(\frac{C}{\Delta V_R}\right)$$

where C is a constant and ΔV_R is the part of the quenched-in free-volume associated with structural relaxation that is recovered during annealing of the glass prior to recrystallization. This is shown schematically in Fig.9.

We propose that during continuing irradiation of an amorphized fuel this excess free-volume is maintained at a value proportional to the damage rate. This results in a commensurate decrease in viscosity, or increase in fluidity, $\phi = \eta^{-1}$, as long as fission events are occurring in the fuel. Likewise, the diffusivity in the fuel that is related to the viscosity through the Nernst-Einstein equation, $D \propto \eta^{-1}$, is enhanced by the magnitude of the fission-induced excess free-volume. It has been shown that the free-volume of a

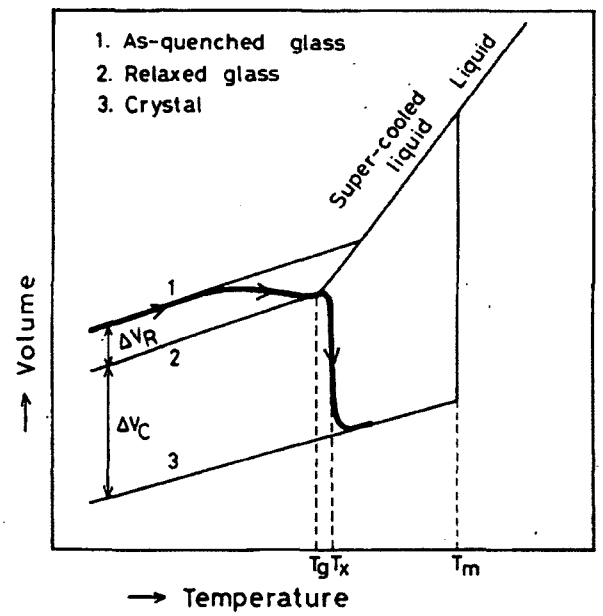

Fig. 9. Schematic Illustration of the Volume-temperature Diagram for Liquid, As-quenched Relaxed Glass and Crystal. ΔV_R and ΔV_C are the Amount of Volume Changed During the Structural Relaxation and Crystallization, Respectively. T_g, T_x and T_m are the Glass Transition, Crystallization and Melting Temperatures, Respectively [35]

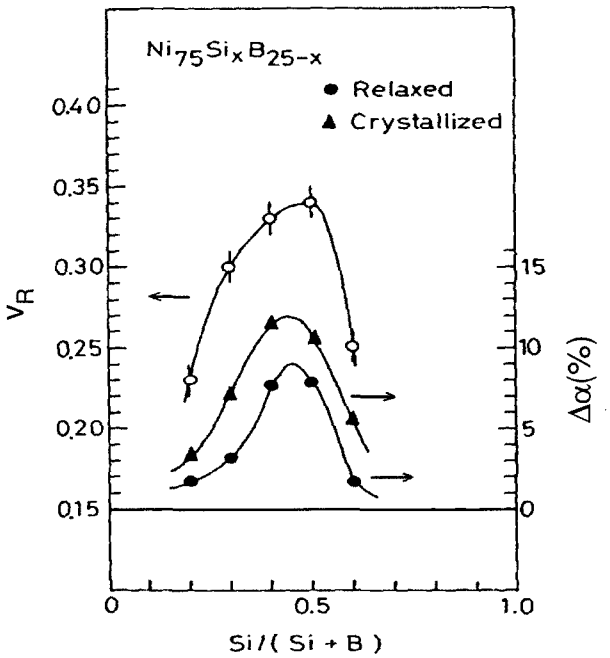

Fig. 10. Effect of Si Content in $Ni_{75}Si_xB_{25-x}$ Metallic Glasses on Free Volume Changes During the Structural Relaxation and Changes ($\Delta \alpha$) In the Thermal Expansion Coefficient in Relaxed and Crystallized Samples [36]

glassy metal is strongly affected by composition, because short range bonding character of an alloy is maintained in the glass state. This is shown for a well known metallic glass in Fig.10 [35]. The effect of composition on the resulting gas bubble behavior of two uranium silicide fuels is shown in Fig.11 [36]. Both U_3Si and U_3Si_2 are amorphized at a low damage dose [37]. Whereas amorphization of U_3Si is accompanied by a relatively large increase in volume, the volume change in U_3Si_2 was found to be negligibly small.

Apparently the additional Si bonds in U_3Si_2 have a large effect on the amount of free-volume in the glassy state, and thereby on the fluidity of the fuel - the fission gas diffusivity – and the resulting swelling behavior. Although amorphization is a prerequisite for low temperature high swelling behavior, it needs to be accompanied by an increase in free volume. The change in fluidity expressed as the overall growth rate per unit dose in displacement-per-atom, dpa, for U_3Si and U_3Si_2 irradiated in a reactor as well as ion beam data by Klaumunzer [38], are shown in Fig.12 to fit the Doolittle equation.

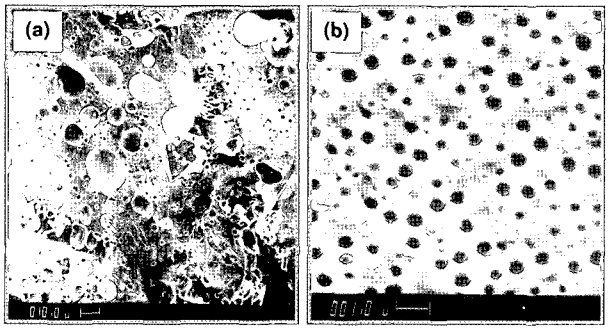

Fig. 11. Influence of Silicon on Amorphous Uranium Silicides; (a) U_3Si (15% total U Burnup), (b) U_3Si_2 19% Total U Burnup). Notice the Difference in Magnification

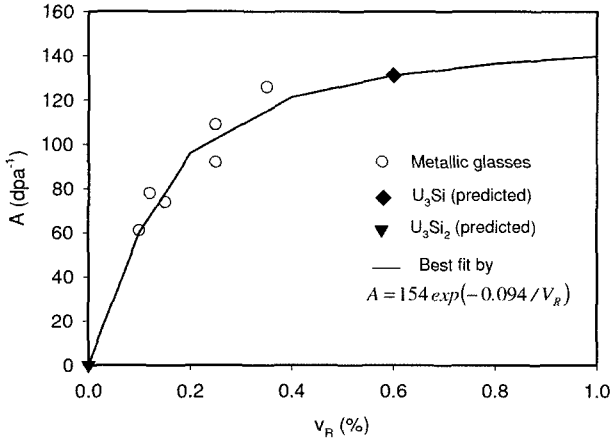

Fig. 12. Growth Rate (A) as a Function of Free Volume (v_R). Data for Metallic Glasses are From [38]

5. CONCLUSION

The development of fission gas porosity in nuclear fuels can be divided into five distinctively different types. Three types of behavior, characterized by anisotropic α-U, cubic ceramic, and high temperature metallic behavior are well-known and have been extensively studied. Less widely known are two equally typical low temperature kinds of fission gas porosity development, viz., one associated with fission induced grain refinement and the other with fission induced amorphization. Crystalline fuel irradiated to high burnup at low temperatures shows grain refinement, whereas amorphous fuel exhibits either breakaway swelling if enough excess free-volume is available or stable swelling if insufficient excess free-volume is present during irradiation.

REFERENCES

[1] W.R. McDonell, "Void model for cavitational swelling of uranium and other anisotropic metals," DP-MS-73-11, Savana River Laboratory (1973).

[2] R.M. Berman, "An x-ray diffraction study of irradiated fluorite-type materials," WAPD-BT-21, Bettis Technical Review. Reactor Technology (1960).

[3] J.D.B Lambert and R. Strain, "Oxide fuels," *Materials Science and Technology*, R.W. Cahn, P. Haasen and E.J. Kramer, Eds., Vol.10A, VCH (1994).

[4] H. Blank, "Nonoxide Ceramic Nuclear Fuels," *Materials Science and Technology*, R.W. Cahn, P. Haasen and E.J. Kramer, Eds., Vol.10A, VCH (1994).

[5] W. Chubb, V.W. Storhok and D.L. Keller, "Obervations relating to the mechanisms of swelling and gas release in uranium dioxide at high temperatures," *J. Nucl. Mater.*, **44**, 136 (1972).

[6] R.M. Berman, "Fission fragment distribution in irradiated UO_2," *Nucl. Sci. Eng.*, **16**, 315 (1963).

[7] J.D.B. Lambert, "Irradiation study of UO_2 - stainless steel and $(Pu,U)O_2$ - stainless steel cermet fuels in rod and plate geometry," *In High Temp. Nucl. Fuels*, A. N. Holden, Ed., P.237, Gordon and Breach (1968).

[8] G.L. Hofman, G.L. Copeland and J.E. Sanecki, "Microscopic investigation into the irradiation behavior of U_3O_8-Al dispersion fuel," *Nucl. Technol.*, **72**, 338 (1986).

[9] C.T. Walker and M. Coquerelle, "Correlation between microstructure and fission gas release in high burnup UO_2 and MOX fuel," *Inter'l Topical Mtg. LWR Fuel Performance, Fuel for the 90s,* p.506, Avignon, France, April 21-24, 1991, Amer. Nucl. Soc. (1991).

[10] H. Stehle, "Performance of oxide nuclear fuel in water-cooled power reactors," *J. Nucl. Mater.*, **153**, 3 (1988).

[11] M.E. Cunningham, M.D. Freshley and D.D. Lanning, "Development and characteristics of the rim region in high burnup UO_2 fuel pellets," *J. Nucl. Mater.*, **188**, 19 (1992).

[12] L.E. Thomas, C.E. Beyer and L.A. Charlot, "Microstructural analysis of LWR spent fuels at high burnup," *J. Nucl. Mater.*, **188**, 80 (1992).

[13] G.L Hofman, M.K. Meyer, J.L. Snelgrove et al., "Initial assessment of radiation behavior of very-high density low-enriched uranium fuels," *The 22nd International Meeting on Reduced Enrichment for Research and Test Reactors*

(*RERTR*), Budapest, Hungary, October 3-8, 1999.
[14] S.J. Thompson and P.E.J. Flewitt, "The defect structure and superconducting transition of cold-worked niobium," *J. Less-Common Metals*, **40(3)**, 269 (1975).
[15] N. Hansen, "Low energy dislocation structures due to unidirectional deformation at low temperatures," *Mater. Sci. Eng.*, **81**, 141 (1986).
[16] C.L. Trybus and W.A. Spitzig, "Chracterization of the strength and microstructural evolution of a heavily cold rolled Cu-20% Nb composite," *Acta Metall.*, **37(7)**, 1971 (1989).
[17] C.L. Trybus, L.S. Chumbley, W.A. Spitzig and J.D. Verhoeven, "Problems in evaluating the dislocation densities in heavily deformed Cu-Nb composites," *Ultamicroscopy*, **30**, 315 (1989).
[18] W.A. Spitzig, C.L. Trybus and F.C. Laabs, "Structure properties of heavily cold-drawn niobium," *Mater. Sci. Eng.*, **A145**, 179 (1991).
[19] J. Rest and G.L. Hofman, "Kinetics of recrystallization and fission-gas-induced swelling in high burnup UO_2 and U_3Si_2 nuclear fuels," *Fundamental Aspects of Inert Gases in Solids*, S.E. Donnelly and J.H. Evans, Eds., p.443, Plenum Press (1991).
[20] J. Rest and G.L. Hofman, "Dynamics of irradiation-induced grain subdivision and swelling in U_3Si_2 and UO_2 fuels," *J. Nucl. Mater.*, **210**, 187 (1994).
[21] J. Rest and G.L. Hofman, "An alternative explanation for evidence that xenon depletion, pore formation, and grain subdivision begin at different local burnups," *J. Nucl. Mater.*, **277**, 231 (2000).
[22] I.L.F. Ray, Hj. Matzke, H.A. Thiele and M. Kinoshita, "An electron microscopy study of the RIM structure of a UO_2 fuel with a high burnup of 7.9% FIMA," *J. Nucl. Mater.*, **245**, 115 (1997).
[23] T. Sonoda, M. Kinoshita, I.L.F. Ray et al., "Transmission electron microscopy observation on irradiation-induced microstructural evolution in high burnup UO_2 disk fuel," *Nucl. Instr. Meth. Phys. Res.*, **B191**, 622 (2002).
[24] K. Nogita and K. Une, "Radiation-induced microstructural change in high burnup UO_2 fuel pellets," *Nucl. Instr. Meth. Phys. Res.*, **B91**, 301 (1994).
[25] A.D. Whapham and B.E. Sheldon, "Radiation damage in uranium dioxide," *Phil. Mag.*, **10**, 1179 (1965).
[26] K. Nogita and K. Une, "Irradiation-induced recrystallization in high burnup UO_2 fuel," *J. Nucl. Mater.*, **226**, 302 (1995).
[27] I.L.F. Ray, H. Thiele and Hj. Matzke, "Transmission electron microscopy study of fission product behavior in high burnup UO_2," *J. Nucl. Mater.*, **188**, 90 (1992).
[28] J. Spino and D. Papaioannou, "Lattice parameter changes associated with the rim-structure formation in high burn-up UO_2 fuels by micro X-ray diffraction," *J. Nucl. Mater.*, **281(2-3)**, 146 (2000).
[29] J. Spino, J. Cobos-Sabate and F. Rousseay, "Room-temperature microindentation behavior of LWR-fuels, part 1: fuel micro-hardness," *J. Nucl. Mater.*, **322**, 204 (2003).
[30] A.D. Whapham and B.E. Sheldon, "Transmission electron microscope study of irradiation effects in sintered uranium dioxide," *J. Nucl. Mater.*, **10**, 157 (1963).
[31] B. Bethune, "Transmission electron microscopy of U3Si-effect of irradiation," *J. Nucl. Mater.*, **40**, 205 (1971).
[32] Mme J. Bloch, "Effet de l'irradiation par les neutrons sur les alliages uranium-fer a faible teneur en fer," *J. Nucl. Mater.*, **6(2)**, 203 (1962).
[33] S. Klaumunzer, "Ion-beam-induced plastic deformation: A universal phenomenon in glasses," *Rad. Effect Defects Solid*, **110**, 79 (1989).
[34] G.S. Grest and M.H. Cohen, "Liquids, glasses and the glass transition: A free-volume approach," *Advances in Chemical Physics*, I. Prigogine and S.A, Price, Eds., John Wiley and Sons, p.469, New York (1981).
[35] T. Komatsu, K. Matusita and R. Yokota, "Volume changes during the structural relaxation and crystallization in Fe-Ni based metallic glasses," *J. Non-crystalline Solids*, **69**, 347 (1985).
[36] T. Komatsu, K. Matusita and R. Yokota, "Quenched-in excess volume and structural relaxation in Fe-Ni based metallic glasses," *J. Non-crystalline Solids*, **85**, 358 (1986).
[37] R.C. Birtcher, J.W. Richardson and M.H. Mueller, "Amorphization of U3Si2 by ion or neutron irradiation," *J. Nucl. Mater.*, **230**, 158 (1996).
[38] S. Klaumunzer, M. Hou, G. Schumacher and C. Li, "Ion-beam induced plastic deformation of amorphous materials," *Proc. Materials Research Society Meeting*, Mar. 1987, Los Angeles, USA (1987).